PERGAMON

Journal of Geodynamics 34 (2002) 193–206

JOURNAL OF
GEODYNAMICS

www.elsevier.com/locate/jgeodyn

Monte Carlo analysis of the latitudinal symmetry of the global buoyancy flux distribution

Douglas H. Oliver

Department of Geological Sciences, Southern Methodist University, Dallas, TX 75275, USA

Abstract

Both the density of terrestrial hot spots and their associated buoyancy flux show non-random distributions. These distributions are bimodal and symmetric about the equator with maxima occurring between 20 and 30° latitude. The buoyancy flux distributions are not an artifact of data bin width or bin spacing. Monte Carlo analysis performed on two independent buoyancy flux estimates shows that the symmetry as measured by the correlation between paired bands of latitude is statistically significant. Excess buoyancy flux in mid-latitude regions has broad implications regarding material and heat flux within the mantle. The Earth's rotation may be a factor in the migration to and/or the generation of excess low-viscosity, thermally buoyant material in mid-latitude regions.

1. Introduction

Hot spots are widely accepted to be the surface expression of mantle plumes and are thought to originate at the core–mantle boundary (CMB) (e.g. Richards et al., 1988, 1991; Sleep, 1992; Walker et al., 1995; Lithgow-Bertelloni and Silver, 1998). The mechanisms by which plumes rise are not well understood and remain controversial. Recent seismic tomography studies of the D″ layer above the CMB (Garnero and Helmberger, 1996; Garnero et al., 1998; Williams et al., 1998; Revenaugh and Meyer, 1997; Lay et al., 1998; Wen and Helmberger, 1998) reveal a thin layer of low-velocity material termed the Ultra Low Velocity Zone (ULVZ). This low-velocity material is thought to have a higher temperature than the overlying mantle and may be partially molten. Because this material is also likely to have lower viscosity, lower density and positive buoyancy relative to the overlying mantle, it may accumulate in specific regions within the D″ layer until it becomes dynamically unstable and rises adiabatically through the mantle. Lateral variations in the thickness of the ULVZ recognized by some workers suggest that accumulations of low-velocity material has occurred in specific locations (Lay et al., 1998; Wen and Helmberger, 1998; Williams

E-mail address: oliver@mail.smu.edu

0264-3707/02/$ - see front matter
PII: S0264-3707(02)00021-2

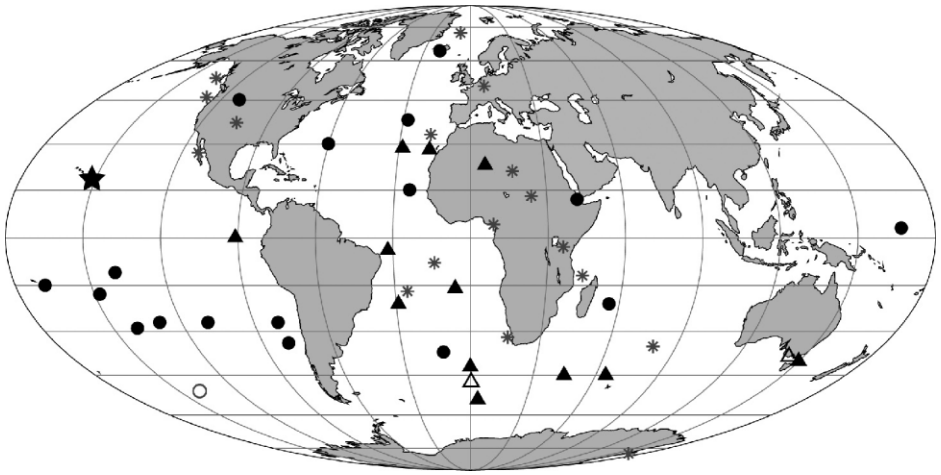

Fig. 1. Global distribution of hot spots. Locations from Richards et al. (1988). Asterisks—hot spots with buoyancy flux of $\leqslant 0.3$ mg/s; triangles—hot spots with buoyancy flux between 0.3 and 1.5 mg/s; circles—hot spots with buoyancy flux between 1.5 and 3.3 mg/sec; star—Hawaii (buoyancy flux of 8.7 mg/s). Open symbols are additional hot spots referenced in Davies (1988).

et al., 1998). Given that the CMB cannot be directly observed, the mechanism(s) driving these accumulations are not well known. In addition, the density and distribution of both earthquakes and observing stations limit the lateral resolution of seismic tomography.

2. Hot spot and flux distributions

A random distribution for hot spots on the Earth's surface would be expected if buoyancy induced by heat transfer from an isothermal outer core across the CMB were the sole driving force for mantle plumes. Previous studies have examined global hot spot distributions by contouring hot spot densities on the surface of the Earth (Duncan and Richards, 1991; Matyska, 1989; Stefanick and Jurdy, 1984), or by expanding the distribution in spherical harmonics (Ribe and de Valpine, 1994). These approaches reveal non-random distributions with hot spot concentrations over certain regions (e.g. Africa, the Pacific Ocean) or in association with low spherical harmonic degrees.

Although it was previously suggested that hot spots are under-represented in polar and equatorial regions, the statistical significance of this distribution was ambiguous (Stothers, 1993). A re-investigation of hot spot distributions was initiated by plotting the number of hot spots per unit area versus latitude for 47 previously identified hot spots (Richards et al., 1988) (Fig. 1). Hot spot densities were determined for 10° bands of latitude from the equator to the poles. The latitudinal distribution of hot spots is bimodal and approximately symmetric about the equator with maxima occurring between 20 and 30° north and south latitudes (Fig. 2a). However, this hot spot density distribution differs little from that reported by Stothers (1993) and, hence, it also lacks statistical significance.

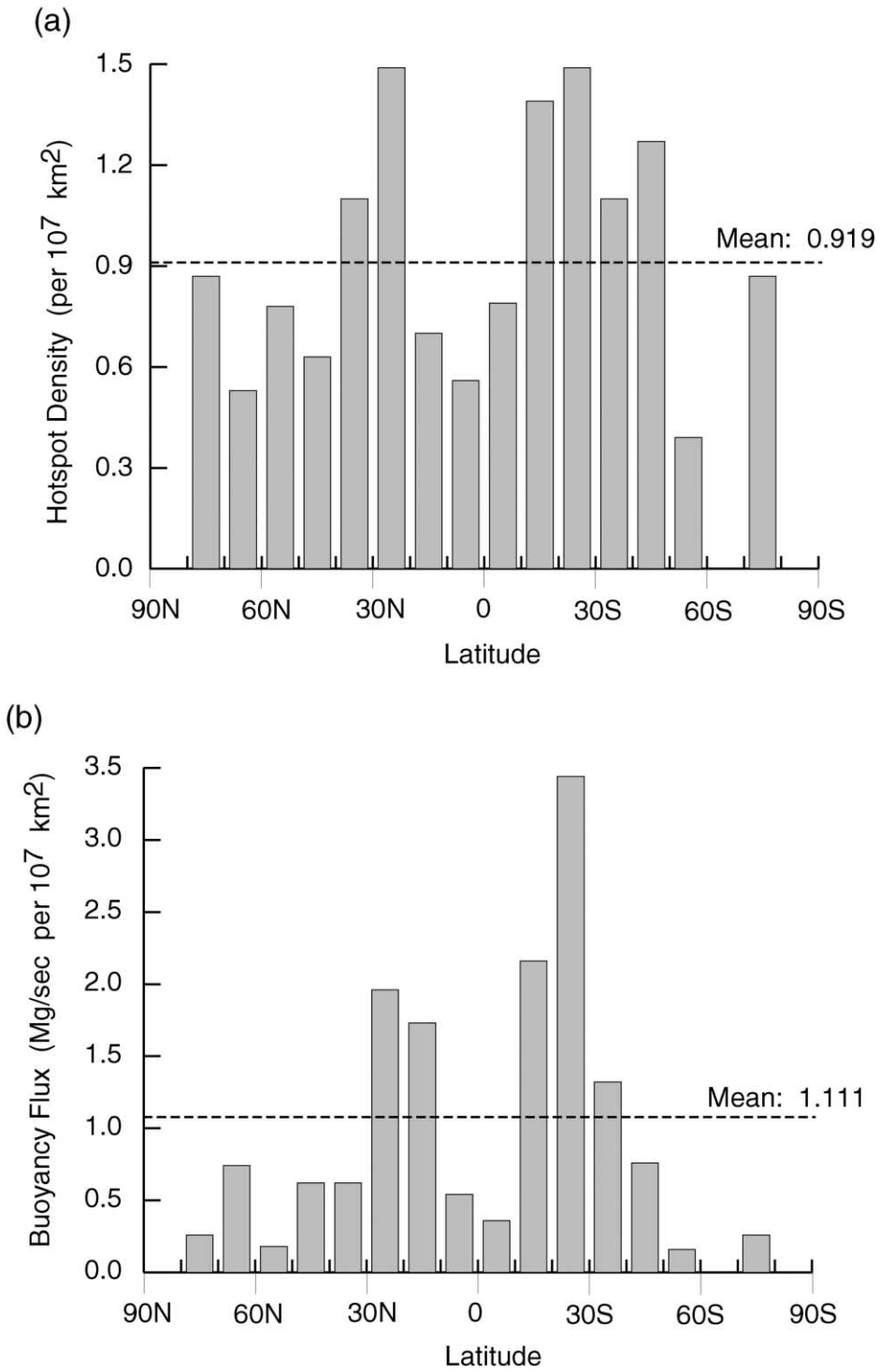

Fig. 2. (a) Density of hot spots per 10^7 km^2 versus latitude. (b) Density of buoyancy flux per 10^7 km^2 versus latitude.

Because the identification of weak hot spots is subjective (e.g. Burke and Wilson, 1976; Crough and Jurdy, 1980; Malamud and Turcotte, 1999), buoyancy flux offers an alternative and more robust method of evaluating hot spot distributions. Weighting hot spots according to their thermal buoyancy minimizes potential bias resulting from the inclusion or omission of weak or poorly defined hot spots because the buoyancy flux associated with ambiguous hot spots is typically small. Using previously determined buoyancy fluxes for the 47 hot spots analyzed above (Sleep, 1990; Ribe and de Valpine, 1994), the buoyancy flux densities for 10° bands of latitude from the equator to the poles were determined (Fig. 2b). The buoyancy flux density distribution is both more strongly bimodal and symmetrical than the hot spot density distributions. The buoyancy flux exceeds the expected value for a uniform distribution by a factor of 1.8 for the northern maximum and 3.1 for the southern maximum. The discrepancy between the northern and southern maxima is further reflected in the hemispherical distribution of buoyancy flux which shows a 42.4–57.6% split between the northern and southern hemispheres, respectively. As a quantitative measure of the symmetry with respect to the equator, the buoyancy flux densities for corresponding bands of latitude in the northern and southern hemispheres were correlated. Earth's buoyancy flux density distribution has a correlation of $+0.915$. In contrast, the hot spot density distribution has a correlation of only $+0.697$, reflecting the higher degree of symmetry in the buoyancy flux distribution.

3. Statistical analysis

Possible explanations for the symmetrical, bimodal buoyancy flux distribution include the possibilities that it is either an artifact of data sorting, a function of the hot spots selected or the fortuitous arrangement of hot spots that are in fact randomly dispersed. The first possibility was evaluated by recalculating the buoyancy flux distributions using various bin widths as well as using a constant 10° latitude spacing but different starting points. The shape of the buoyancy flux distributions show that the binning scheme has little effect on the outcome. Whereas the different bin widths change the amplitude of the maxima (Fig. 3a), the locations of the maxima do not change appreciably. More important, the key characteristics of the distribution—the bimodal and symmetrical morphology—remain intact. The effect of changing the starting point for a constant 10° latitude spacing is also negligible (Fig. 3b).

The effect of including misidentified hot spots was tested by recalculating the buoyancy flux distributions using only the hot spots with the strongest buoyancy flux. Potentially misidentified hot spots are likely to be the ones with the smallest buoyancy flux (e.g. Raton, Bowie, Mt. Erebus). Because the buoyancy flux associated with Earth's hot spots approximates a power-law distribution (Malamud and Turcotte, 1999), the key characteristics of the buoyancy flux density distribution should not be significantly altered by excluding the weakest hot spots. The effect of excluding the 16 hot spots with buoyancy fluxes of $\leqslant 0.3$ mg/s was to reduce the buoyancy flux correlation from $+0.915$ to $+0.888$. Excluding the 25 hot spots of with buoyancy fluxes of $\leqslant 0.5$ mg/s resulted in a correlation of $+0.865$. This demonstrates that although the weak hot spots contribute to the observed symmetry in the buoyancy flux distribution, the relationship is not dependant on them.

Evaluating the possibility that a fortuitous yet random hot spot placement has produced the observed bimodal and symmetrical buoyancy flux distribution involved the use of Monte Carlo

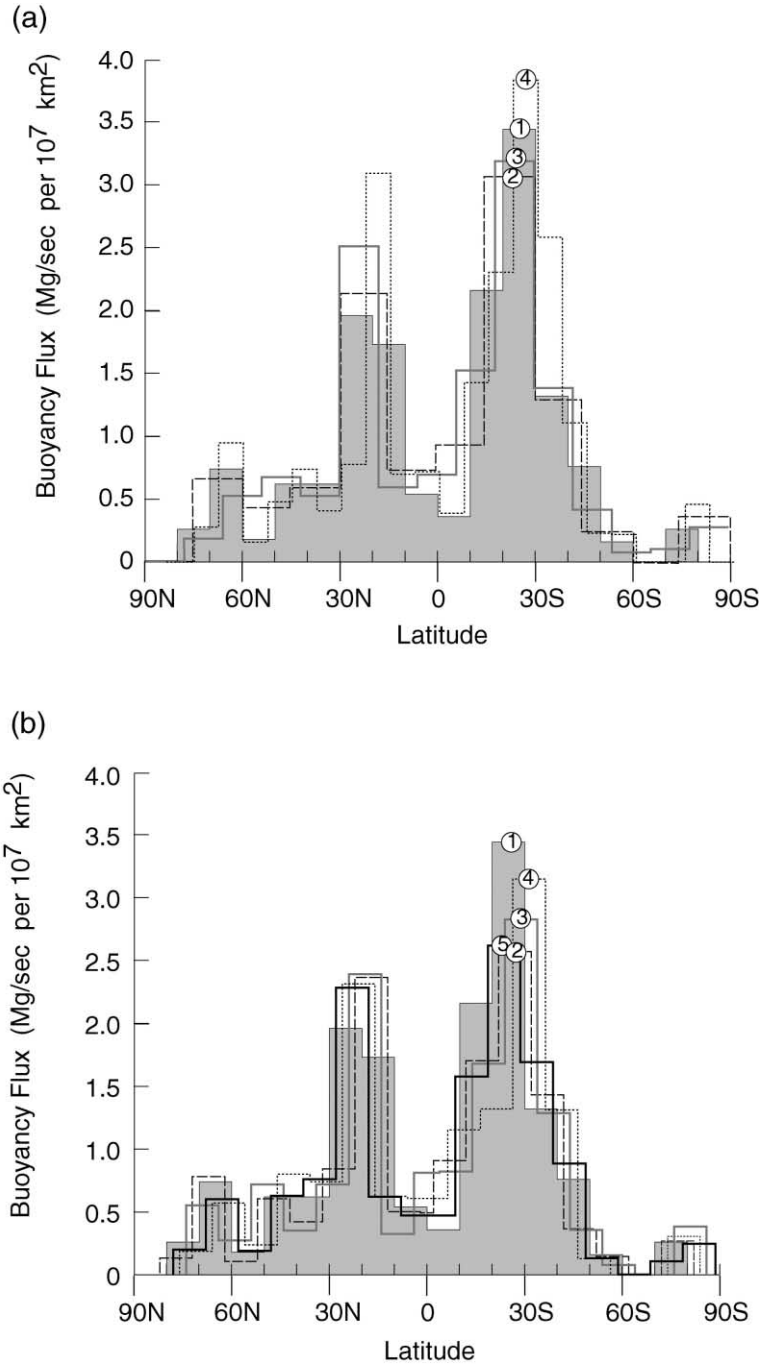

Fig. 3. (a) Density of hot spots per 10^7 km^2 versus latitude using different bid widths starting at the equator. 1–10° bin width (solid gray), 2–12° bin width, 3–15° bin width, 4–7.5° bin width. (b) Density of buoyancy flux per 10^7 km^2 versus latitude using a constant 10° bin width with different starting points. 1—Starting point of 0° N and S (solid gray), 2—starting points of 2° N and S, 3—starting points of 4° N and S, 4—starting points of 6° N and S, 5—starting points of 8° N and S.

analysis. Key features of the observed buoyancy flux distribution include the magnitude of the maxima relative to a uniform distribution, the sub-equal buoyancy flux in the northern and southern hemispheres, and the symmetry of the buoyancy flux relative to the equator as measured by the high positive correlation between corresponding bands of latitude in opposite hemispheres. Monte Carlo analysis was used to evaluate the statistical significance of these parameters. Forty-seven hot spots with the same distribution of buoyancy fluxes as those currently observed were randomly redistributed on a spherical surface. Buoyancy flux densities were determined for 10° bands of latitude starting at the equator for the new hot spot distributions. The results were evaluated for the presence and amplitude of maxima, for the percentage of total flux in each hemisphere, and for symmetry as measured by the correlation coefficient between buoyancy flux densities in corresponding bands of latitude in opposite hemispheres. A total of 2000 iterations were performed.

The results from the Monte Carlo analysis indicate that the amplitude of Earth's observed buoyancy flux maxima are not significant—the existence of a few hot spots having very strong fluxes (e.g. Hawaii, Tahiti, Marquesas) virtually precludes a uniform flux distribution. Similarly, the sub-equal distribution between the two hemispheres in the observed buoyancy flux was commonly reproduced through the Monte Carlo analysis. Approximately 46% of the iterations had flux distributions at least as evenly distributed as what is observed on Earth. However, the symmetry of Earth's buoyancy flux distribution as measured by the high positive correlation coefficient is more significant. Only 6 of the 2000 iterations resulted in correlation coefficients with a higher positive value. The correlation coefficients generated by the Monte Carlo analysis show a skewed normal distribution with a mean of $+0.030$ and a standard deviation of 0.368 (Fig. 4a). Based on this mean and standard deviation, Earth's observed correlation of $+0.915$ is significant at a $>99\%$ confidence level for a one-tailed distribution. This effectively eliminates the possibility that the observed symmetry in Earth's buoyancy flux is random.

The Monte Carlo analysis described above was repeated using a second independent estimate of buoyancy flux determined by Davies (1988). Because Davies (1988) calculated buoyancy fluxes for only 26 hot spots, flux estimates determined by Sleep (1990) and Ribe and de Valpine (1994) were used for those hot spots not analyzed. In addition, three hot spots not considered by Richards et al. (1988) but analyzed by Davies (1988) (East Australia, Louisville and Meteor) were included bringing the total to 50. The observed correlation coefficient of $+0.847$ is somewhat lower than that previously determined using the flux estimates of Sleep (1990). The lower correlation coefficient is largely the result of adding three hot spots all in the southern hemisphere which already has an excess buoyancy flux relative to the northern hemisphere. However, the buoyancy flux density distribution using Davies (1988) values is still characterized by maxima between 20 and 30° latitude and symmetry with respect to the equator. The results of the Monte Carlo analysis are also broadly similar to those previously described. The correlation coefficients show the same skewed normal distribution with a mean of $+0.034$ and a standard deviation of 0.382 (Fig. 4b). Based on this mean and standard deviation, the correlation coefficient of $+0.847$ using Davies (1988) buoyancy flux estimates is significant at a $>98\%$ confidence level for a one-tailed distribution.

Few of the iterations with the highest positive correlation coefficients show the coherent symmetry observed in Earth's buoyancy flux distribution (Fig. 5a–j). The apparent symmetry for many of the iterations with high positive correlations is achieved through the placement of a few

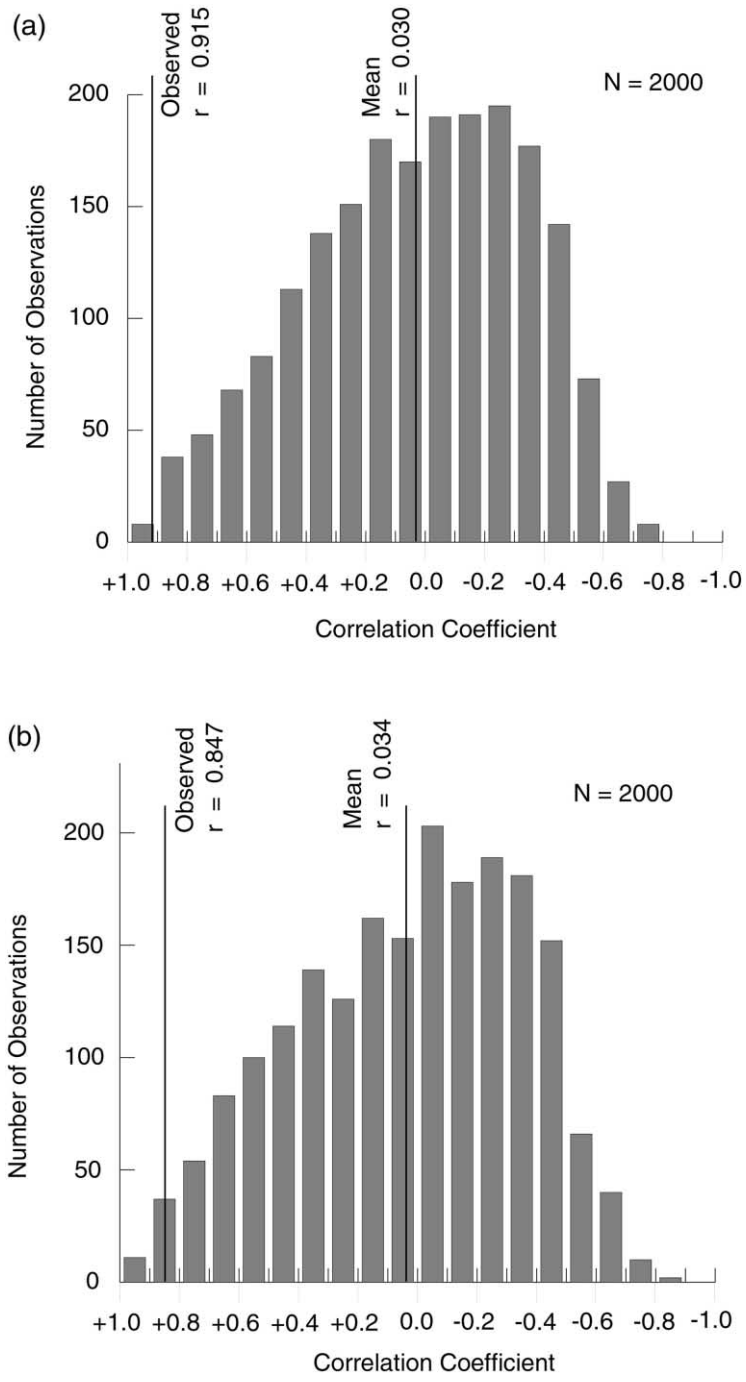

Fig. 4. (a) Distribution of correlation coefficients for Monte Carlo analysis using buoyancy flux estimates of Sleep (1990) and Ribe and de Valpine (1994). (b) Distribution of correlation coefficients for Monte Carlo analysis using buoyancy flux estimates of Davies (1988). Estimates of Sleep (1990) and Ribe and de Valpine (1994) were used for hot spots not analyzed by Davies (1988).

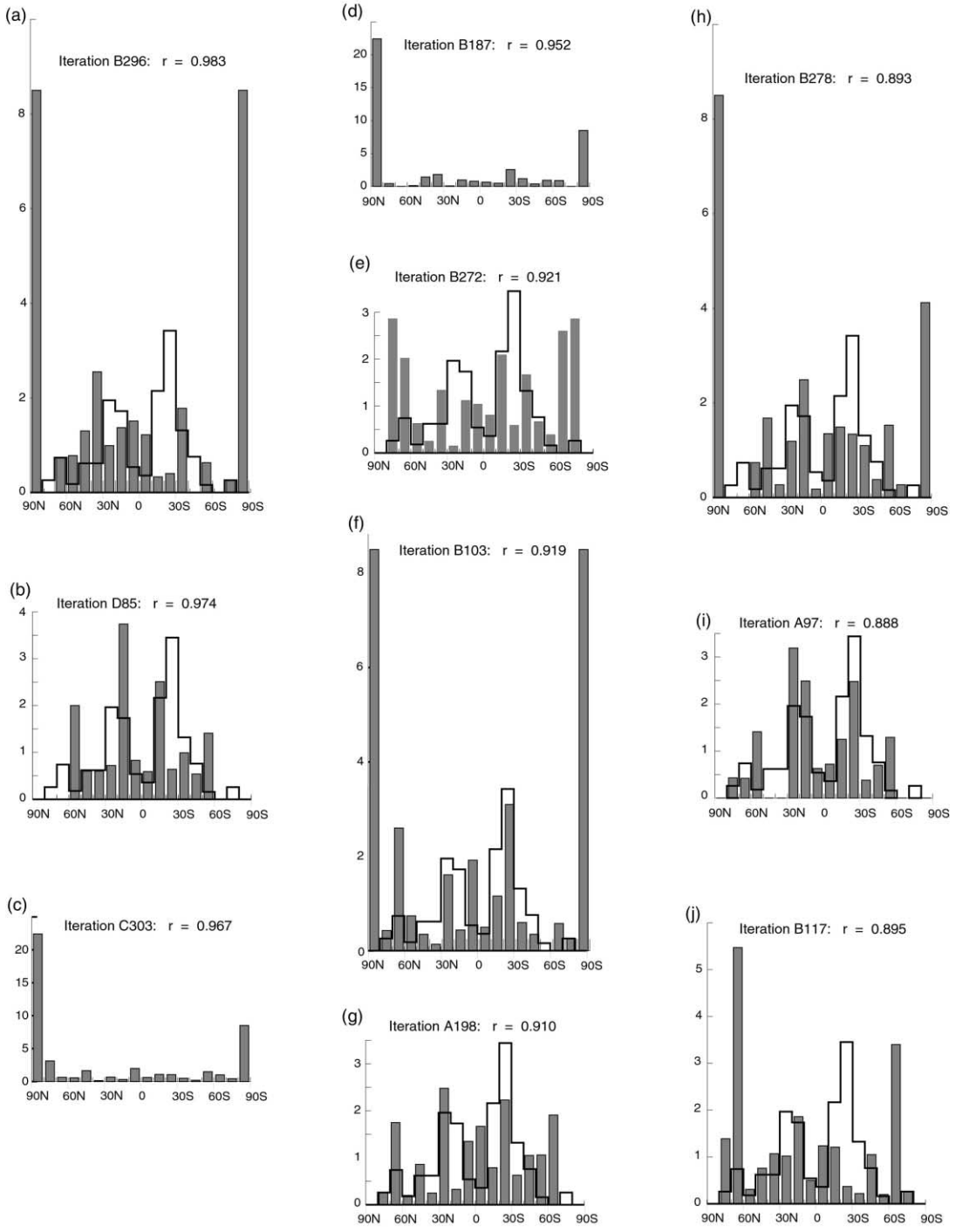

Fig. 5. Density of buoyancy flux per 10^7 km^2 versus latitude for the Monte Carlo iterations having the highest positive correlation coefficients. Black line represents Earth's observed buoyancy flux distribution. Iterations (c) and (d) are not to scale.

strong hot spots in both polar regions which results in very large buoyancy flux densities for those areas (Fig. 5a, c, d, f, h and j). Other strong correlations lack a coherent symmetry and consist of equivalent buoyancy fluxes in corresponding bands of latitude in opposite hemispheres that appear to be randomly distributed (Fig. 5e, g and i). Consequently, the distribution plots suggest that the Monte Carlo analysis may actually underestimate the statistical significance of the high degree of symmetry observed in Earth's buoyancy flux distribution.

4. Discussion

The geographic distribution of hot spots may be governed in part by plume-lithosphere interactions, plate motions or mantle convection. In addition to providing a possible explanation for the clustering of hot spots in specific geographic areas, these factors may also be reflected in Earth's buoyancy flux distribution to some extent. The southern hemisphere's greater buoyancy flux may be a function of the disproportionate continental area in the northern hemisphere, and may reflect the relative ease with which buoyant material rising beneath hot spots penetrates oceanic versus continental lithosphere. However, none of these factors provides a plausible explanation for the hot spot and buoyancy flux maxima between 20 and 30° latitude, nor for the symmetry of these distributions relative to the equator.

Whereas thermal, compositional, and/or mechanical heterogeneities in the source region (i.e. CMB characteristics) may also govern hot spot distributions, it is unlikely that these factors can produce the observed coherent global distribution. Similarly, a random hot spot and/or buoyancy flux distribution is expected for buoyancy induced solely by heat transfer across the CMB. Topographic irregularities in the D″ layer (e.g. Jeanloz and Lay, 1993; Wysessions, 1996; Jeanloz and Romanowicz, 1993) may serve as "drip points" thus localizing buoyant material for the nascent mantle plumes, however their influence would be restricted to their immediate area. Consequently, the flux maxima and symmetry in Earth's buoyancy flux distribution may indicate that previously unsuspected processes operating deep within the Earth are at work.

Because the symmetry occurs in the buoyancy flux distribution for the whole Earth, the processes required to explain the observed distribution must also operate on a global or regional rather than local scale. Earth's observed buoyancy flux can be achieved by either the migration of hot, low-viscosity material within the D″ layer from polar and/or equatorial areas to mid-latitudes (Fig. 6a), or by excess heating beneath the CMB in mid-latitudes (or conversely by cooling in polar and/or equatorial areas) providing additional thermal buoyancy to the base of the overlying mantle (Fig. 6b). The buoyant material, whether transported to or generated in the mid-latitude portions of the CMB, then rises through the mantle beneath existing hot spots.

The excess buoyancy flux between 20 and 30° latitude has broad implications regarding material and heat flux within the deep Earth. The buoyancy flux distribution is consistent with a scenario where buoyant material generated above the CMB flows within the D″ layer to hot spots which act as conduits to the surface. Depending on the effective migration distance for the buoyant material, this may provide an alternative mechanism to mantle convection for cycling material from the base of the mantle to the surface in mid-latitude regions. This alternative material transfer process within the mantle would not operate in polar regions where buoyancy flux is weak. Consequently, the disproportionate buoyancy flux may provide a mechanism for

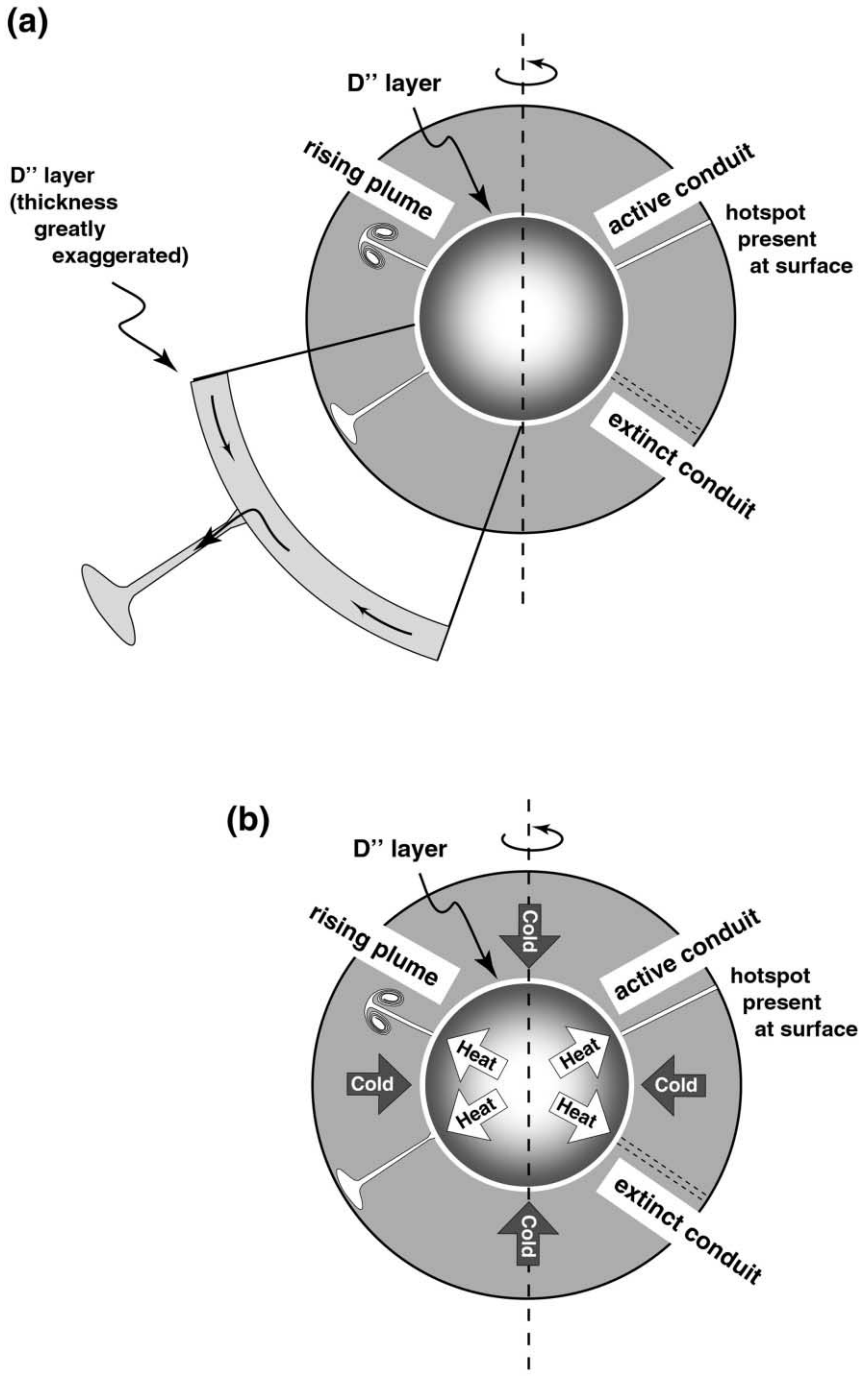

Fig. 6. Global models for hot spot distributions. (a) Low-viscosity material migrates from polar and/or equatorial regions within the D″ layer to mid-latitude regions. (b) Excess heating along the base of the CMB in mid-latitude regions produces thermally buoyant material. Low-viscosity and/or thermally buoyant material either accumulates until it reaches the critical volume for plume lift-off or drains upward through conduits beneath existing hot spots.

creating compositional and isotopic heterogeneities within the lower mantle. The rise of buoyant material will also affect the thermal budget of the overlying mantle as well as the CMB. Heat transfer from buoyant material rising through the hot spot conduits into the surrounding mantle will result in elevated mantle temperatures at mid-latitudes. Seismic tomography studies reveal slower mantle P-wave velocities at mid-latitudes relative to equatorial or polar regions which is consistent with elevated temperatures (Glukhovskii and Moralev, 1998). Heat transfer from buoyant material rising from the D″ layer through the adjacent mantle at mid-latitudes may be responsible for this reduction in P-wave velocities. In addition, the observed buoyancy flux distribution likely significantly underestimates the total buoyancy flux arriving in mid-latitude regions when averaged over long periods of time. The buoyancy flux estimates consider only the flux contribution from the residual hot spots and not the mantle plumes that preceded them. Although the duration of interaction between a plume head and the Earth's surface is short-lived compared to that of a hot spot, the annual heat flux associated with the plume is necessarily orders of magnitude greater. Consequently, a sizable component of the total flux is effectively ignored.

Because the observed distribution is symmetric with respect to the equator (i.e. the plane normal to the rotation axis), it is possible that the observed buoyancy flux distribution may be at least in part related to the Earth's rotation. The distribution of possible buoyancy-related features on other bodies in the Solar System is consistent with a rotation-related mechanism. Earth and Mars have comparable periods of rotation (24 versus 24.6 h, respectively). On Mars, the large volcanoes in the Tharsis rise and Elysium are considered to be the products of hot spots impinging on the base of the Martian lithosphere (Hartmann, 1973; Plescia and Saunders, 1982). Because Mars presumably lacks a mobile aesthenosphere and therefore plate tectonics, these hot spots remain stationary with respect to the surface and are very long-lived features (Tanaka, 1986). Although buoyancy flux constraints for the volcanoes on Mars are lacking, they show an axisymmetric distribution similar to that observed on Earth (Matyska et al., 1998). The volcanoes are located in mid- to low-latitudes, albiet primarily in the northern hemisphere. Coronae on Venus, characterized by circular topographic surface expressions, associated rifts and abundant lava flows, are also interpreted to be the product of mantle diapirs (Squyres et al., 1992; Stofan et al., 1992). Although the distribution of Venusian coronae is non-random (Stefanick and Jurdy, 1996), they differ from terrestrial hot spots in that their distribution does not show a latitudinal symmetry (Fig. 7). The extremely slow rotation period for Venus (one complete revolution in $\sim$243 Earth days) is consistent with the hypothesis that rotation is an important factor in determining hot spot distributions. Because corona likely originate at mid-mantle depths rather than the CMB (Smrekar and Stofan, 1999), they may not be ideal analogs to terrestrial hot spots. However, a key similarity is that both young coronae and terrestrial hot spots show a strong correlation with residual geoid highs (Crough and Jurdy, 1980; Jurdy and Stefanick, 1999). Finally, sunspots also show a geographic distribution remarkably similar to that of Earth's buoyancy flux (Stothers, 1993, Fig. 4). Although there is nothing to suggest that sunspots represent buoyancy-related features, they are considered surface manifestations of deep Solar mantle convection (Spruit et al., 1990; Stothers, 1993). The Sun has a period of rotation of $\sim$25 days near the equator and $\sim$30 days near the poles.

Attempts to elucidate a driving mechanism compatible with what is generally accepted regarding outer core and CMB dynamics were unsuccessful. The effects of both centrifugal force and

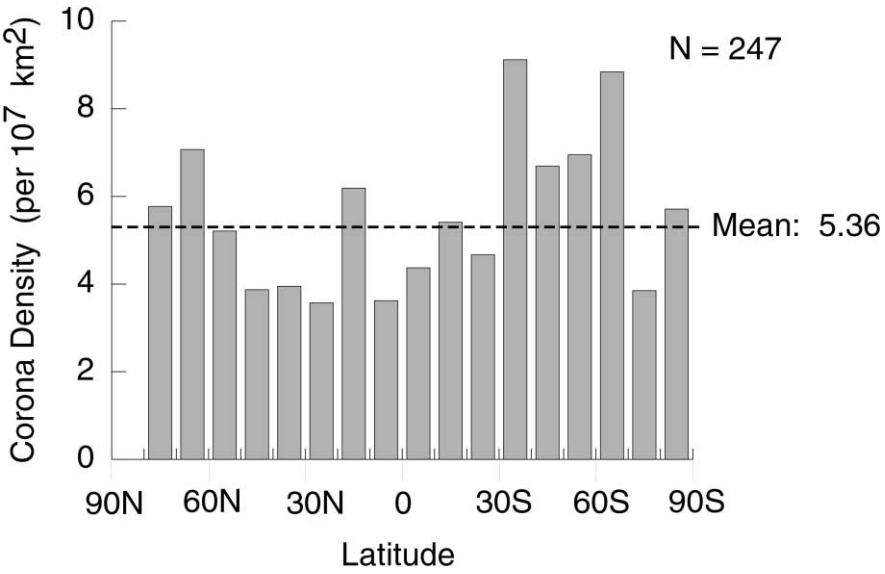

Fig. 7. Density of corona per 10^7 km^2 versus latitude for Venus.

secondary flow induced by differential rotation were examined, however neither provided a satisfactory solution. Although the Earth's buoyancy flux distribution remains an unexplained observation, it is also a constraint that must be accommodated in any model that attempts to explain the dynamics of hot spots and the initiation of mantle plumes. More important, it is an indication that undefined processes may be at work within the deep Earth—processes that involve not only material and heat flux in the CMB region, but also interactions between the deep Earth and its surface.

Acknowledgements

This paper grew out of a graduate seminar at Southern Methodist University. The author wishes to acknowledge Vicki Hansen, Rebecca Ghent, Jason Head and Crayton Yapp for helpful discussions. Donna Jurdy, Norm Sleep and Paul Stoddard are thanked for constructive reviews.

References

Burke, K.C., Wilson, J.T., 1976. Hot spots on the Earth's surface. Scientific American 235, 46–57.

Crough, S.T., Jurdy, S.T., 1980. Subducted lithosphere, hot spots and, the geoid. Earth and Planetary Science Letters 48, 15–22.

Davies, G.F., 1988. Ocean bathymetry and mantle convection: 1. Large-scale flow and hot spots. Journal of Geophysical Research 93, 10467–10480.

Duncan, R.A., Richards, M.A., 1991. Hot spots, mantle plumes, flood basalts, and true polar wander. Review Geophysics 29, 31–50.

Garnero, E.J., Helmberger, D.V., 1996. Seismic detection of a thin laterally varying boundary layer at the base of the mantle beneath the central-Pacific. Geophysical Research Letters 23, 977–980.
Garnero, E. J., Revenaugh, J., Williams, Q., Lay, T., Kellogg, L., 1998. Ultra-low velocity zone at the core-mantle boundary. In: Gurnis, M. et al., (Eds.), The Core-Mantle Boundary Region. American Geophysical Union Geodynamics 28, pp. 319–334.
Glukhovskii, M.Z., Moralev, V.M., 1998. The hot belt of the early Earth and present-day mantle geodynamics according to seismic-tomography data. Russian Geology and Geophysics 39, 1–7.
Hartmann, W.K., 1973. Martian surface and crust: review and synthesis. Icarus 19, 550–575.
Jeanloz, R., Lay, T., 1993. The core-mantle boundary. Scientific American 268, 48–55.
Jurdy, D.M., Stefanick, M., 1999. Correlation of Venus surface features and geoid. Icarus 139, 93–99.
Jeanloz, R., Romanowicz, B., 1993. Geophysical dynamics at the center of the Earth. Physics Today 50, 22–27.
Lay, T., Williams, Q., Garnero, E.J., 1998. The core-mantle boundary layer and deep Earth dynamics. Nature 392, 461–468.
Lithgow-Bertelloni, C., Silver, P.G., 1998. Dynamic topography, plate driving forces and the African superswell. Nature 395, 269–272.
Malamud, B.D., Turcotte, D.L., 1999. How many plumes are there? Earth and Planetary Science Letters 174, 113–124.
Matyska, C., 1989. Angular symmetries of hot spot distributions. Earth and Planetary Science Letters 95, 334–340.
Matyska, C., Yuen, D.A., Breuer, D., Spohn, T., 1998. Symmetries of volcanic distribution on Mars and Earth and their mantle plume dynamics. Journal of Geophysical Research 103, 28587–28597.
Revenaugh, J., Meyer, R., 1997. Seismic evidence of partial melt within a possibly ubiquitous low-velocity layer at the base of the mantle. Science 277, 670–673.
Plescia, J.B., Saunders, R.S., 1982. Tectonic history of the Tharsis region, Mars. Journal of Geophysical Research 87, 9775–9791.
Ribe, N.M., de Valpine, D.P., 1994. The global hot spot distribution and instability of D″. Geophysical Research Letters 21, 1507–1510.
Richards, M.A., Hager, B.H., Sleep, N.H., 1988. Dynamically supported geoid highs over hot spots: observations and theory. Journal of Geophysical Research 93, 7690–7708.
Richards, M.A., Jones, D.L., Duncan, R.A., DePaolo, D.J., 1991. A mantle plume initiation model for the Wrangellia flood basalt and other oceanic plateaus. Science 254, 263–267.
Sleep, N.H., 1990. Hot spots and mantle plumes: some phenomenology. Journal of Geophysical Research 95, 6715–6736.
Sleep, N.H., 1992. Hot spot volcanism and mantle plumes. Annual Reviews of Earth and Planetary Science 20, 19–43.
Smrekar, S.E., Stofan, E.R., 1999. Origin of corona-dominated topographic rises on Venus. Icarus 139, 100–115.
Spruit, H.C., Nordlund, A., Title, A.M., 1990. Solar convection. Annual Reviews of Astronomy and Astrophysics 28, 263–301.
Squyres, S.W., Janes, D.M., Baer, G., Bindschadler, D.L., Schubert, G.R., Sharpton, V.L., Stofan, E., 1992. The morphology and evolution coronae on Venus. Journal of Geophysical Research 97, 13611–13634.
Stefanick, M., Jurdy, D.M., 1996. The distribution of hot spots. Journal of Geophysical Research 89, 9919–9925.
Stefanick, M., Jurdy, D.M., 1996. Venus coronae, craters amnd chasmata. Journal of Geophysical Research 101, 4637–4643.
Stofan, E.R., Sharpton, V.L., Schubert, G., Baer, G., Bindschadler, D.L., Janes, D.M., Squyres, S.W., 1992. Global distribution of corona and related features on Venus: implications for origin and relation to mantle processes. Journal of Geophysical Research 97, 13347–13378.
Stothers, R.B., 1993. Hot spots and sunspots: surface tracers of deep mantle convection in the Earth and Sun. Earth and Planetary Science Letters 116, 1–8.
Tanaka, K.L., 1986. The stratigraphy of Mars. Journal of Geophysical Research 91, E139–E158.
Walker, R.J., Morgan, J.W., Horan, M.F., 1995. Osmium-187 enrichment in some plumes: evidence for core-mantle interaction? Science 269, 819–822.
Wen, L., Helmberger, D.V., 1998. Ultra-low velocity zones near the core-mantle boundary from broadband PKP precursors. Science 279, 1701–1703.

Williams, Q., Revenaugh, J., Garnero, E.J., 1998. A correlation between ultra-low basal velocities in the mantle and hot spots. Science 281, 546–549.
Wysession, M.E., 1996. Large-scale structure at the core-mantle boundary from diffracted waves. Nature 382, 244–248.